

**GRID-SEARCH LOCATION METHODS FOR GROUND-TRUTH COLLECTION
FROM LOCAL AND REGIONAL SEISMIC NETWORKS**

William L. Rodi,¹ Stephen C. Myers,² and Craig A. Schultz²

Massachusetts Institute of Technology;¹ Lawrence Livermore National Laboratory²

Sponsored by National Nuclear Security Administration
Office of Nonproliferation Research and Engineering
Office of Defense Nuclear Nonproliferation

Contract No. DE-FC03-01SF22397¹ and W-7405-ENG-48²

ABSTRACT

The objective of this project is to develop improved seismic event location techniques that can be used to generate more and better quality reference events using data from local and regional seismic networks. Our approach is to extend existing methods of multiple-event location with more general models of the errors affecting seismic arrival time data, including picking errors and errors in model-based travel-times (path corrections). Toward this end, we are integrating a grid-search based algorithm for multiple-event location (GMEL) with a new parameterization of travel-time corrections and new kriging method for estimating the correction parameters from observed travel-time residuals. Like several other multiple-event location algorithms, GMEL currently assumes event-independent path corrections and is thus restricted to small event clusters. Our new parameterization assumes that travel-time corrections are a function of both the event and station location, and builds in source-receiver reciprocity and correlation between the corrections from proximate paths as constraints. Our new kriging method simultaneously interpolates travel-time residuals from multiple stations and events to estimate the correction parameters as functions of position. We are currently developing the algorithmic extensions to GMEL needed to combine the new parameterization and kriging method with the simultaneous location of events. The result will be a multiple-event location method that is applicable to non-clustered, spatially well-distributed events. We are applying the existing components of our new multiple-event location method to a dataset of regional and local arrival times from Nevada Test Site (NTS) explosions with known origin parameters. Preliminary results show the feasibility and potential benefits of combining our location and kriging techniques. We also show some preliminary work on generalization of the error model used in GMEL with the use of mixture-of-Gaussians probability distributions fit to observed travel-time residuals.

OBJECTIVE

Multiple-event location methods are enjoying increased popularity as tools for calibration and ground-truth collection (e.g. Engdahl and Bergman, 2001). The objective of this project is to develop improved multiple-event location techniques that can be used to increase the number and accuracy of reference events obtained from local and regional seismic networks. The limitations of existing methods can be primarily attributed to their parameterization of path travel-time corrections and the prior information allowed on these corrections. Typically, path corrections are assumed to be event-independent, which limits the location method to small event clusters, and unrelated between stations, which misses an important constraint when closely separated stations are involved. We are extending an existing multiple-event location algorithm (GMEL) to incorporate a more general model of path corrections and new procedures for estimating the corrections from multiple-station data. Further, existing event location methods are generally limited to Gaussian models of observational (picking) errors, therefore, we are investigating a more general error model parameterized with mixtures of Gaussians that can accommodate skewed and multi-modal error distributions.

RESEARCH ACCOMPLISHED

Approach

Multiple-event location problem

To describe our approach we consider the basic multiple-event location problem involving only first P arrival times observed for a subset of paths between m events ($i=1,2\dots m$) and n stations ($j=1,2\dots n$). This problem can be stated as

$$d_{ij} = t_i + T_j(\mathbf{x}_i) + c_{ij} + e_{ij} \quad (1)$$

where d_{ij} is the observed arrival time for the (i, j) th path; t_i and \mathbf{x}_i are origin parameters (time and hypocenter, respectively) of the i th event; T_j is a model-based travel-time function for the j th station; c_{ij} is a correction to this function; and e_{ij} is an observational (picking) error in d_{ij} . The unknowns in this inverse problem are the event parameters, (\mathbf{x}_i, t_i) , and the path corrections, c_{ij} . As part of the multiple-event location problem we may include appropriate prior constraints on the unknown parameters.

Path corrections

Multiple-event location methods (e.g., Dewey, 1971; Jordan and Sverdrup, 1981; Pavlis and Booker, 1983) have generally assumed that the path corrections are event-independent, i.e.

$$c_{ij} = a_j \quad (2)$$

where a_j is a time term associated with the j th station. This assumption is also made by GMEL. The inverse problem then becomes to solve simultaneously for the m event hypocenters $(\mathbf{x}_1, t_1, \mathbf{x}_2, t_2, \dots, \mathbf{x}_m, t_m)$ and the n station time terms (a_1, a_2, \dots, a_n) . GMEL accomplishes this with an iterative procedure for alternatively updating event hypocenters and station time terms, employing a grid-search technique for locating the events (see Rodi et al., 2002a). The use of a grid search makes it straightforward to constrain parameters within specified bounds, allowing the incorporation of ground-truth (GT) constraints on event locations.

The assumption of event-independent path corrections restricts our multiple-event location method to events with cluster sizes that are small compared to the cluster's distance to stations. This imposes a severe restriction on the event-station geometries that can be used in the multiple-event analysis, e.g. disallowing stations too close to the event cluster.

The more general parameterization of path corrections we are pursuing extends the idea of Schultz et al. (1998), which is to allow an explicit dependence on the location of an event, i.e.

$$c_{ij} = C_j(\mathbf{x}_i). \quad (3)$$

Our extension allows an explicit dependence on both the event *and* station locations. Denoting the latter as \mathbf{y}_j , for the j station, we have

$$c_{ij} = C(\mathbf{x}_i, \mathbf{y}_j). \quad (4)$$

The multiple-event location problem then becomes to solve simultaneously for the m event hypocenters and the function $C(\mathbf{x}, \mathbf{y})$.

Since the function C has an infinite number of degrees of freedom, it is necessary to either restrict its functional form or invoke strong smoothness constraints on its spatial dependence, or both. To restrict the functional form of C we parameterize it in terms of one or more *universal parameter* functions, which are not specific to a particular event or station. The simplest such parameter function is a *time-term* function, a , which yields the correction for a path as

$$C(\mathbf{x}, \mathbf{y}) = a(\mathbf{x}) + a(\mathbf{y}). \quad (5)$$

It is clear that the time-term function generates reciprocal travel-time corrections, since the event location \mathbf{x} and station location \mathbf{y} can be interchanged in equation (5). A more flexible parameterization, employed in the examples shown later, is a *mislocation-vector* function, $\mathbf{a}(\mathbf{x})$, for which

$$C(\mathbf{x}, \mathbf{y}) = \mathbf{p}(\mathbf{x}, \mathbf{y}) \cdot \mathbf{a}(\mathbf{x}) + \mathbf{q}(\mathbf{x}, \mathbf{y}) \cdot \mathbf{a}(\mathbf{y}). \quad (6)$$

Here, \mathbf{p} is the gradient of the model-based travel-time with respect to the event location, while \mathbf{q} is the gradient with respect to the station location:

$$\mathbf{p} = \nabla_1 T(\mathbf{x}, \mathbf{y}) \quad (7)$$

$$\mathbf{q} = \nabla_2 T(\mathbf{x}, \mathbf{y}). \quad (8)$$

(∇_k means gradient with respect the k th argument of a function.) Each is a slowness vector pointed in the direction of the raypath, and each depends on both \mathbf{x} and \mathbf{y} since the raypath depends on the location of both its endpoints. The interpretation of \mathbf{a} as a mislocation vector follows from the fact that equation (6) is the first order change in travel-time that results from perturbing the event location by $\mathbf{a}(\mathbf{x})$ and the station location by $\mathbf{a}(\mathbf{y})$.

Since T is a reciprocal function of its arguments, we have $\mathbf{p}(\mathbf{x}, \mathbf{y}) = \mathbf{q}(\mathbf{y}, \mathbf{x})$, which shows that the mislocation-vector parameterization also generates travel-time corrections that are source-receiver reciprocal.

We point out that station-specific correction functions of the type considered by Schultz et al. (1998) are easily defined in terms of universal parameter functions. In the case of the mislocation-vector parameterization:

$$a_j(\mathbf{x}) = \mathbf{p}(\mathbf{x}, \mathbf{y}_j) \cdot \mathbf{a}(\mathbf{x}) + \mathbf{q}(\mathbf{x}, \mathbf{y}_j) \cdot \mathbf{a}(\mathbf{y}_j). \quad (9)$$

This points up an important advantage of universal parameterizations such as those above. They define a correction function for a station at any location, whether or not the station has observed travel-time residuals to constrain the function. This is accomplished by allowing correlations between the corrections among stations and between stations and events.

We are developing an extension of GMEL that will solve simultaneously for m event locations and a universal parameter function that generates path corrections. The algorithm will alternate between two processes: locating events with the parameter functions fixed, and interpolating travel-time residuals with the event locations fixed. The latter process solves an interpolation problem that involves residuals from all the stations. To date, we have developed an algorithm, known as *multiple-station kriging*, to solve this interpolation problem but we have not yet integrated it with our multiple-event location algorithm.

Multiple-station kriging

We describe our new kriging algorithm for the simpler case of the time-term parameter function, $a(\mathbf{x})$, although the applications below use the mislocation-vector parameter, $\mathbf{a}(\mathbf{x})$, of equation (6).

For given event locations, we can define the set of residuals from the observed paths as

$$r_{ij} = d_{ij} - t_i - T_j(\mathbf{x}_i). \quad (10)$$

The interpolation problem for the time-term function then becomes

$$r_{ij} = a(\mathbf{x}_i) + a(\mathbf{y}_j) + e_{ij}. \quad (11)$$

This problem can be solved with geo-statistical constraints, as used in conventional kriging. However, we adopt a maximum-likelihood (ML) approach to the inverse problem, instead of the minimum-variance approach used in conventional kriging (e.g. Deutsch and Journel, 1998). For Gaussian data errors, the ML approach takes the solution of (11) to be the function a that minimizes the objective function given by

$$\chi^2 = \sum_{ij} |r_{ij} - a(\mathbf{x}_i) - a(\mathbf{y}_j)|^2 / \sigma_{ij}^2 + \int a(\mathbf{x}) [D a](\mathbf{x}) d\mathbf{x} \quad (12)$$

where σ_{ij} is the assigned standard deviation of e_{ij} and D is a specified differential operator. The maximum-likelihood inversion approach is equivalent to conventional kriging with a given correlation function when D is the *inverse* of the *covariance* operator that corresponds to the correlation function. That is, the covariance operator is the Green's function for the differential operator.

Currently we use the following operator for kriging in N spatial dimensions ($N = 1, 2$ or 3):

$$D = \frac{\text{const}}{\sigma_0^2} \left(\frac{1}{2\ell} \frac{\partial^2}{\partial x^2} + L_x^2 \frac{\partial^2}{\partial y^2} + L_y^2 \frac{\partial^2}{\partial z^2} \right) \quad (13)$$

where σ_0^2 is a prior variance of the parameter function and L_x , L_y and L_z are correlation lengths in the x , y and z directions of a local Cartesian coordinate system. Various choices of the operator order, ℓ , correspond to correlation functions that are commonly used in conventional kriging, e.g. the *exponential* correlation function ($\ell = 1$ in 1-D, $\ell = 2$ in 3-D) and Gaussian correlation function ($\ell = 2$). While we have expressed this operator in Cartesian coordinates, we have actually implemented it as a difference operator in a global, spherical coordinate system. We solve the ML criterion ($\chi^2 = \text{minimum}$) for a sampled version of the function a on a latitude/longitude/depth grid. Numerically, the minimization is performed with a conjugate gradients technique.

Application to Nevada Test Site

We are applying our new approach to a dataset from the NTS explosions that have been assembled by Lawrence Livermore National Laboratory (LLNL) (Walter et al., 2003). The dataset comprises 74 nuclear explosions with known locations and origin times recorded at a network of regional and local stations. A LLNL analyst re-picked the phases and supplemented them with selected picks from the National Earthquake Information Center (NEIC) to produce a high quality dataset. The dataset has been used in studies of event location accuracy at LLNL (Myers et al., 2003) and we are using it to test our new approach to multiple-event location and kriging. The examples here use only the Pn picks from the dataset and we removed events with fewer than four Pn arrivals. The resulting subset comprises 674 arrivals from 71 events and 59 stations.

We applied the multiple-station kriging approach to the NTS data to estimate a universal parameter function of the mislocation-vector type. Depth dependence was not allowed since all the events are shallow. However, we note that the path travel-time corrections derived from the parameter function will be depth dependent owing to the depth-dependence of the slowness vectors in equation (6).

Multiple-station kriging

In these initial tests, we applied our kriging method to travel-time residuals using the IASP91 tables for model-based times and using the ground-truth locations of the events. We tried various values of the geo-statistical input parameters, as follows. In each case the order of the correlation operator ($\ell = 2$, see equation (13)) was set to 2. In 2-D, this corresponds to a correlation function that is peaked at zero distance, but less peaked than a correlation function of the exponential type. We show the results for two combinations of the prior error on the mislocation function (\square_0) and the correlation distance ($L = L_x = L_y$). Figure 1 shows the mislocation function obtained with $\square_0 = 5$ km and $L = 200$ km, while Figure 2 shows the functions obtained with $\square_0 = 10$ and $L = 100$. The results are similar, but the smaller correlation distance and larger prior error (Figure 2) results in a rougher function with somewhat larger values, especially in the east component. This second case also fits the travel-time residuals better, yielding a 0.428 sec posterior RMS compared to 0.455 for the first case. The prior RMS of the residuals was 0.922 sec.

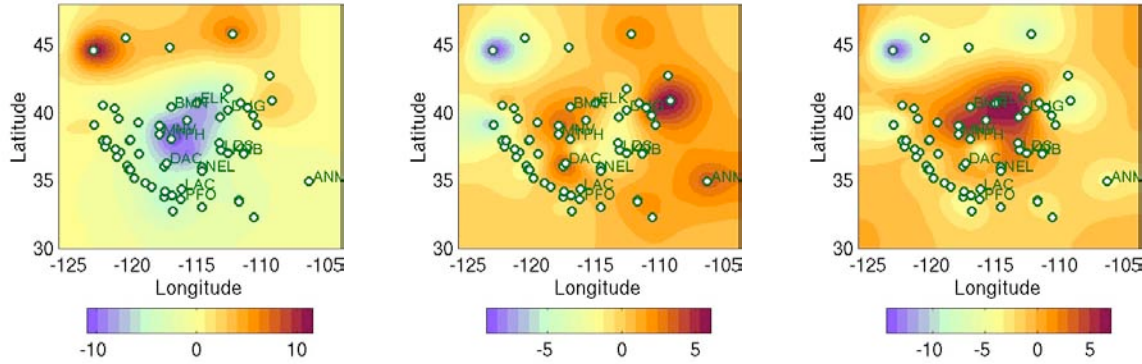


Figure 1: 2-D mislocation-vector parameter function for the region surrounding NTS: north, east and depth components (left, middle and right panels, respectively). This parameter function was derived by multiple-station kriging of Pn travel-time residuals, using 200 km for the correlation distance and 5 km for the prior error on the mislocation components. Station locations (some labeled) are marked with circles.

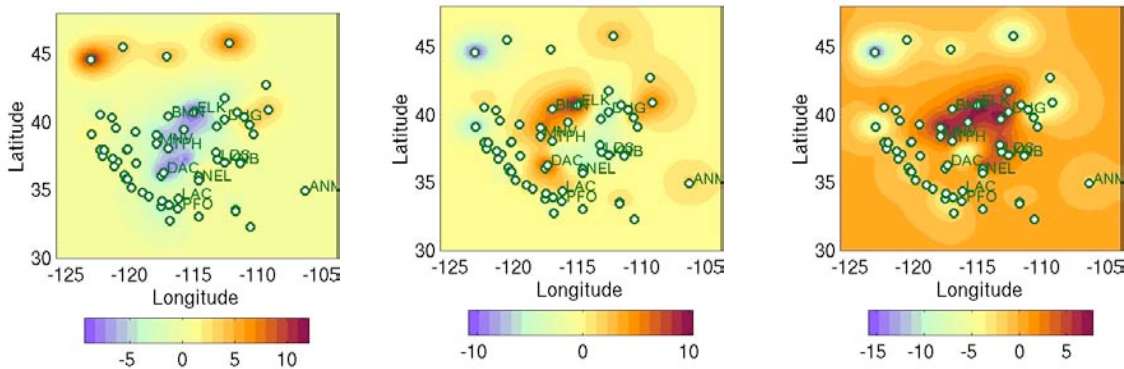


Figure 2: Same as Figure 1 but the mislocation-vector function was obtained using 100 km for the correlation distance and 10 km for the prior error on the mislocation components.

Next we show some travel-time correction functions generated from the second parameter function. Figure 3 shows the correction functions for stations ELK and BMN. These two stations are north of NTS and close to one another, and we see that their travel-time corrections are very similar (highly correlated). Figure 4 displays the correction functions for KNB, a station east of NTS, and LAC, south of NTS. Their pattern of corrections shows significant differences from each other and from the northern stations.

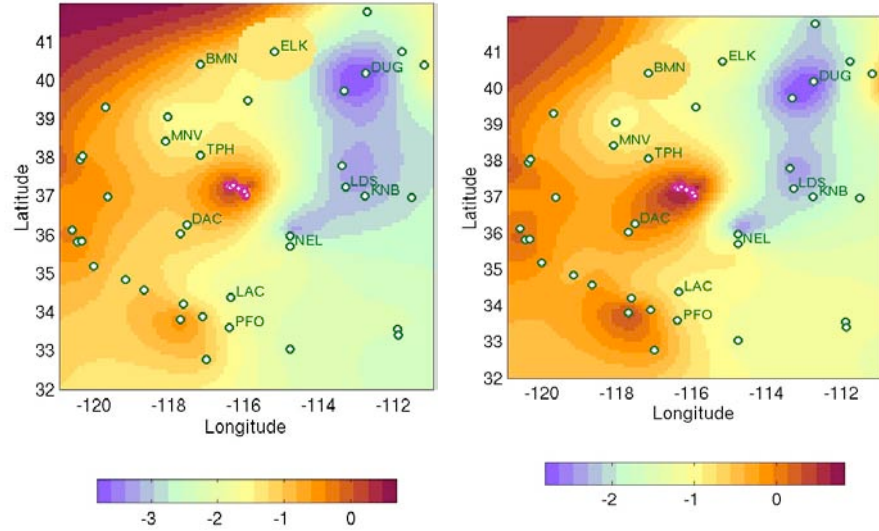


Figure 3: Travel-time correction functions for stations ELK (left) and BMN (right), generated from the 2-D mislocation-vector parameter function shown in Figure 2. The functions are displayed for zero event depth. Station locations (some labeled) are marked with circles, and the NTS events show as a small cluster of small white dots near the center of the plot.

Location experiments

We show some experiments with single-event and multiple-event location that compare the location accuracy achieved with various types of path corrections. First, we compare single-event location solutions using fixed path corrections, i.e. the events are located individually with no changes to the specified path corrections. Three cases of path corrections were used in this way:

1. Zero path corrections.
2. Station time-term corrections, obtained by averaging the residuals obtained using the ground-truth locations.
3. Travel-time correction functions obtained from the ground-truth residuals (examples are Figures 3 and 4).

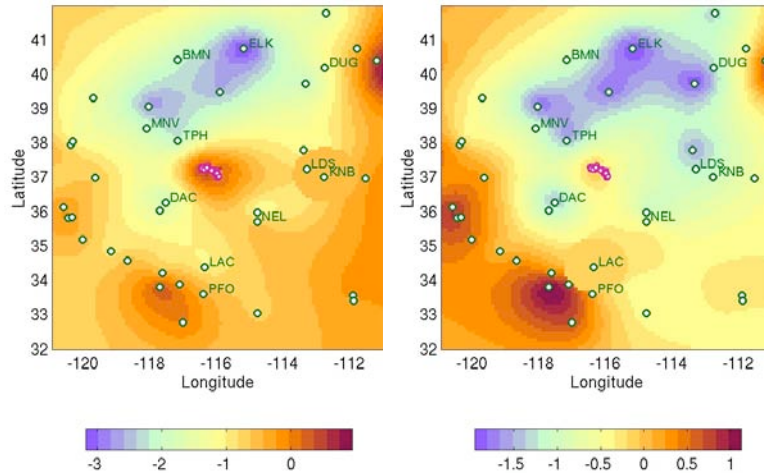


Figure 4: Travel-time correction functions for stations KNB (left) and LAC (right), generated from the 2-D mislocation-vector parameter function shown in Figure 2.

In each case, the dataset comprised 674 Pn arrivals from 71 events. Locations were run with depth bounded between 0 and 50 km.

Table 1 summarizes the location accuracy achieved with the various types of path corrections. The two versions obtained from kriged correction functions refer to the different correlation parameters used; A and B correspond to Figures 1 and 2, respectively. The table shows only epicenter mislocations, but we note that depth mislocations were often significant since only Pn arrivals were used. We see from the table that all versions of travel-time corrections improve location accuracy significantly, compared to zero corrections (line 1). The number of events with mislocations greater than 5 km drops from 15 to 3 when corrections are used in the location process. We also see that the mislocations obtained using kriged correction functions are somewhat better than those using station time terms. We point out that, in this application, the event aperture is small (approx. 50 km). Therefore, the main difference between correction terms and correction functions is that the latter allow for correlation between stations, based on their separation, while station terms are independent between stations regardless of their separation. Figure 5 shows the actual event locations obtained for two of the four cases in the table: zero corrections (line 1) and kriged corrections B (line 5).

Table 1. Location Accuracy of NTS Events: Comparison of Path Corrections.

Corrections Used	No. of Events vs. Misloc.				Largest Misloc. (km)
	<1	1–3	3–5	>5	
None	4	38	14	15	10.4
station terms	27	38	3	3	9.8
kriged correction function (A)	36	29	3	3	9.4
kriged correction function (B)	40	26	2	3	9.1

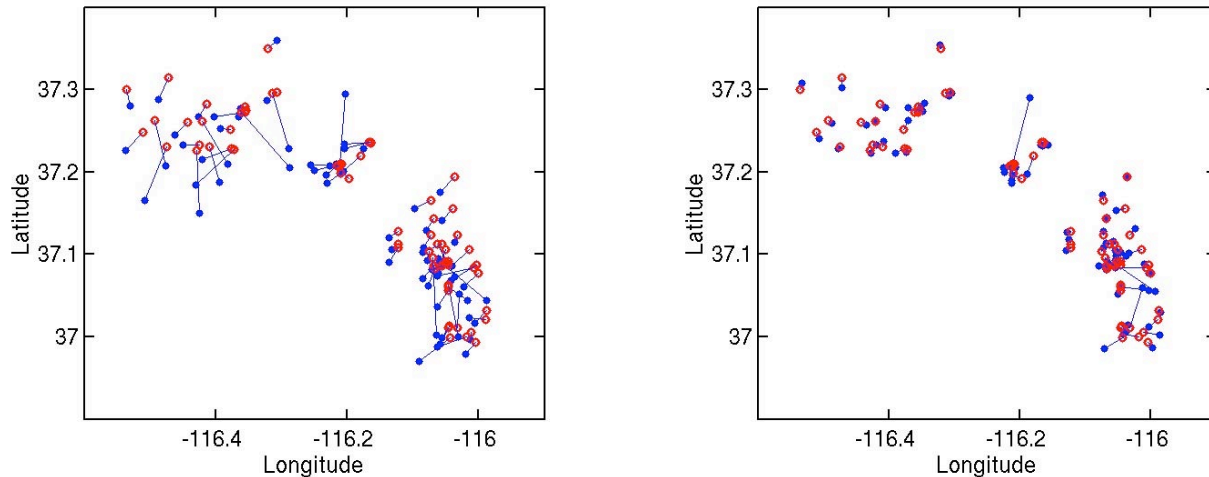


Figure 5: Locations and mislocations resulting from single-event location applied with no station corrections (left) and travel-time correction functions derived from multiple-station kriging, version B (right). In each panel, the filled (blue) circles are the solutions obtained with the location procedure and the unfilled (red) circles are ground-truth locations. A line connects the solution and GT location of each event.

We emphasize that both types of corrections just compared were derived from travel-time residuals computed using ground-truth locations for all the events, which is not realistic. In practice the corrections must be derived using limited ground-truth information. To see what difference this makes, Table 2 compares location results obtained with the ground-truth version of station terms (line 1) with those obtained using only one ground-truth location in a multiple-event location solution that solves simultaneously for the station time terms. (Note that line 1 of Table 2 repeats line 2 of Table 1.) We see from Table 2 that when there is only one ground-truth location (the best recorded event, at Rainier Mesa), the mislocations are increased, although it is mainly the smallest mislocations that get worse. The largest mislocations are similar.

Table 2. Location Accuracy of NTS Events: Single- vs. Multiple-Event Location.

Loc. Method	No. of Events vs. Misloc.				Largest Misloc. (km)
	<1	1–3	3–5	>5	
Single (with GT0 station terms)	27	38	3	3	9.8
Multiple (with one GT0 constraint)	12	46	11	2	8.9

Since we have not yet integrated our multiple-station kriging method into GMEL, we do not know how well correction functions will do when derived with limited ground-truth information. We do not expect a degradation from those with station terms and correction functions will accommodate large event clusters, whereas the station term approach breaks down.

Extended Error Model

This aspect of our project addresses the complex error processes that affect arrival time measurements, as discussed in Rodi et al. (2002b). The error model now used in GMEL accepts non-Gaussian probability distributions for picking errors, but only of a restricted class (generalized Gaussian) that does not include asymmetrical (skewed) or multi-modal distributions. We are pursuing an alternative class of error distributions known as mixtures, or weighted sums, of Gaussian distributions having different means and variances.

We have developed an algorithm for fitting mixtures of Gaussians to an observed set of travel-time residuals. Given the number of terms in the mixture, K , the algorithm finds the weight, mean and variance of each component Gaussian distribution such that the sum provides the best fit to the histogram of observed residuals. Given the best fitting parameters for each K , the remaining task is to choose the smallest K that can explain, but not over fit, the data. Our algorithm for fitting the Gaussian parameters is a Markov-Chain Monte Carlo (MCMC) technique that optimizes the RMS misfit between the mixture distribution and the observed histogram.

Figure 6 shows an example of fitting mixtures-of-Gaussian distributions to observed residuals from the 1991 Racha earthquake sequence. The left panel shows a single Gaussian function fit to the observed histogram of residuals and the right panel is the best fitting mixture of five Gaussians, which is able to represent the multi-modal nature of the observations.

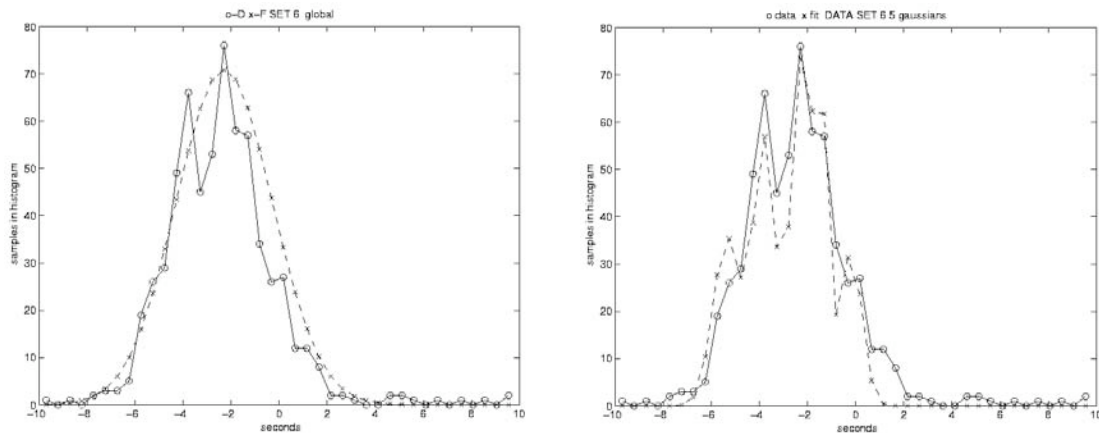


Figure 6: Probability distributions (dashed lines) fit to an observed histogram of travel-time residuals (solid line). The observed residuals are from the Racha earthquake sequence. *Left*: a single Gaussian distribution is fit to the data. *Right*: a mixture of five Gaussians is fit.

CONCLUSIONS AND RECOMMENDATIONS

We have developed and tested the key components of a new multiple-event location method that will allow the use of spatially well-distributed events and take into account correlations between the path travel-time corrections from proximate event-station paths, that are based on the spatial separation between their end-points. Preliminary tests of these components on a high quality dataset from NTS explosions, with known locations, indicate that our approach promises to improve location accuracy over single-event methods in more general station and event geometries than current methods of multiple-event location. Thus, our approach has the potential to provide more high quality reference events needed in calibration studies.

REFERENCES

- Deutsch, C.V. and A.G. Journel (1998). *GSLIB: Geostatistical Software Library and User's Guide*, 2nd ed., Oxford University Press, Inc., New York, 369 pp.
- Dewey, J.W. (1971). Seismicity studies with the method of joint hypocenter determination, *Ph.D. Thesis*, University of California, Berkeley.
- Engdahl, E.R. and E.A. Bergman (2001), Validation and generation of reference events by cluster analysis, *Proceedings, 23rd Seismic Research Review: Worldwide Monitoring of Nuclear Explosions*, Jackson Hole, Wyoming.
- Jordan, T.H. and K.A. Sverdrup (1981). Teleseismic location techniques and their application to earthquake clusters in the south-central Pacific, *Bull. Seism. Soc. Am.*, 71, 1105-1130.
- Myers, S.C., D.B. Harris, M.L. Anderson, W.R. Walter, M.P. Flanagan and F. Ryall (2003). LLNL location and detection research, *Proceedings of the 25th Seismic Research Review*, Tucson, Arizona, this volume.
- Pavlis, G.L. and J.R. Booker (1983). Progressive multiple event location (PMEL), *Bull. Seism. Soc. Am.* 73, 1753-1777.
- Rodi, W., E.R. Engdahl, E.A. Bergman, F. Waldhauser, G.L. Pavlis, H. Israelsson, J.W. Dewey and M.N. Toksöz (2002a). A new grid-search multiple-event location algorithm and a comparison of methods, "Proceedings of the 24th Seismic Research Review: Nuclear Explosion Monitoring: Innovation and Integration", 2002, Los Alamos National Laboratory LA-UR-02-5048., Ponte Vedra Beach, Florida, 403-411.
- Rodi, W., C.A. Schultz, W.G. Hanley, S. Sarkar and H.S. Kuleli (2002b). Grid-search location methods for ground-truth collection from local and regional seismic networks, "Proceedings of the 24th Seismic Research Review: Nuclear Explosion Monitoring: Innovation and Integration", 2002, Los Alamos National Laboratory LA-UR-02-5048. Ponte Vedra Beach, Florida, 394-402.
- Schultz, C.A., S.C. Myers, J. Hipp and C.J. Young (1998). Nonstationary Bayesian kriging: a predictive technique to generate spatial corrections for seismic detection, location, and identification, *Bull. Seism. Soc. Am.*, 88, 1275-1288.
- Walter, W.R., K. D. Smith, J. L. O'Boyle, T. F. Hauk, F. Ryall, S.D. Ruppert, S.C. Myers, M. Anderson, and D.A. Dodge (2003), Improving the fundamental understanding of regional seismic signal processing with a unique western United States dataset, *Proceedings of the 25th Seismic Research Review*, Tucson, Arizona.